Syntheses and x-ray crystal structures of $[MoO(SCH_2CH_2CH_2S)_2]^-$ and $[Mo_2O_2(\mu\text{-}N_3)(SCH_2CH_2CH_2S)_3]^-$. A study of the redox behaviour of $[MoO(SCH_2CH_2S)_2]^-$ by cyclic voltammetry using convolution analysis

Peter T. Bishop and Jonathan R. Dilworth

Department of Chemistry and Biological Chemistry, University of Essex, Colchester C04 3SQ, UK

John P. Hutchinson and Jon A. Zubieta

Department of Chemistry, State University of New York at Albany, N.Y. 12222, USA

Summary

The complexes $[PPh_4][MoO\{S(CH_2)_nS\}_2]$, n = 2 *(1)* n = 3 *(3)*, were synthesised from the Mo^{VI} dioxo-precursor complex $[MoO_2$(butane-2,3-diolato)$_2]$ and the appropriate thiol in the presence of base. Complex *(3)* exhibits a square pyramidal geometry. Crystal Data: $P2_{1/n}$, Z = 4, a = 9.612(2), b = 21.202(4), c = 15.462(3) Å, β = 103.06(1)°, V = 3043.3 Å^3, F(000) = 1364.0, 3687 reflections collected, and 1957 used in solution with R = 0.058. $[MoO(SCH_2CH_2CH_2S)_2]^-$ reacts with hydrazoic acid in methanol to produce $[Mo_2O_2(\mu\text{-}N_3)(SCH_2CH_2CH_2S)_3]$ *(5)*, crystal data: $P_{2_12_12_1}$ a = 9.398(3), b = 14.650(2), c = 27.42(2) (Å), $\alpha = \beta = \gamma = 90°$, Z = 4 V = 3775.8 Å^3, F(000) = 1872.0, 2563 reflections collected and 1244 were used in the solution with R = 0.058. The complex is an asymmetric dimer with a triple bridge comprising two dithiolate sulphurs and a nitrogen of the azide ligand. Convolution analysis of the cyclic voltammetric response of complex *(1)* confirmed a diffusion controlled one electron reversible reduction process.

Introduction

The chemical, spectroscopic[1], and structural[2] properties of $[PPh_4][MoO(SPh)_4]$ have been extensively studied. This complex exhibits square pyramidal geometry with an apical, terminally coordinated oxo-ligand. It was initially hoped we could utilize the Mo=O moiety to synthesise molybdenum thiolato-complexes containing multiply-bonded nitrogen ligands by condensation-type reactions. However, it was found that 1,1-disubstituted hydrazines reacted with $[MoO(SPh)_4]^-$ to give compounds of the type $[MoO(NNR_2)(SPh)_3]^-$ with perferential removal of a thiolate ligand[3].

By using chelating alkyl dithiols it was hoped that the chelate effect would prevent thiolate loss and that simple condensation-type reactions of the Mo=O group would occur. Although the structural properties of $[MoO(SCH_2CH_2S)_2]^-$ [4] and $[MoO(SCH_2CH_2CH_2S)_2]^-$ [5] have briefly been reported, their reactivity has not been included. This paper details the synthesis, redox and structural properties of some mononuclear molybdenum(V) oxo-dithiolate complexes and their reactions with hydrazoic acid.

Results and discussion

Synthesis of $[MoO\{S(CH_2)_nS\}_2]^-$, *n = 2 or 3*

Monomeric oxo-dithiolate complexes of molybdenum can be prepared from the reaction of the butane-2,3-diolato-complex $[MoO_2\{(Me)CHOHCHO(Me)\}_2]$ with an excess of dithiolato-anion (generated *in situ* from the dithiol and triethylamine) in methanol. Spectroscopic, analytical and physical data for complexes *(1)*→*(4)* are listed in Table 1.

Previous attempts to synthesise complexes *(1)*→*(4)* using $[MoOCl_3(thf)_2]$ were unsuccessful[6], but synthesis of $[MoO(SCH_2CH_2S)_2]^-$ has been reported by reaction of $[MoO(SPh)_4]^-$ with the dithiolate[4]. Utilising the *cis*-oxo butanediolato-precursor we found these compounds could be isolated rapidly in good yield (*ca.* 70%). They precipitate from methanol as purple-blue microcrystalline solids by addition of an appropriate cation and are soluble in acetonitrile or dichloromethane. The solutions bleach when allowed to stand for protracted times in air. Complexes *(1)*→*(3)* are 1:1 electrolytes and *(4)* is a 2:1 electrolyte (in *ca.* 0.1 M acetonitrile solutions). They are all paramagnetic, consistent with the molybdenum atom having a formal oxidation state of +5 with one unpaired electron. Their e.p.r. spectra have been discussed elsewhere[4].

The i.r. spectra of complexes *(1)*→*(4)* all show a sharp intense band at *ca.* 930 cm^{-1} which is assigned to the terminally co-ordinated oxo-ligand. These values are identical to that found in $[MoO(SPh)_4]^-$ [3] and lower than that of $[MoOCl_4]^-$ (1020 cm^{-1})[7] and reflect the enhanced electron donating ability of the thiolate ligand compared to that of chloride.

The u.v. spectra (acetonitrile solutions) are all dominated by intense peaks around 500–600 nm (Table 1). The responsible transitions are likely to be ligand to metal charge transfer in origin for the following reasons:- First, the magnitude of the molar extinction coefficients and the ligand dependence of λ_{max} with displacement to higher frequency as the ligand becomes more electron donating, ($^-S(CH_2)_2S^- \rightarrow {}^-S(CH_2)_3S^-$). Secondly, analogous ligand to metal charge transfer bands are also present in the u.v. spectrum of the $[MoO(SPh)_4]^-$ anion and its derivatives[1].

Synthesis of $[Mo_2O_2(\mu\text{-}N_3)(SCH_2CH_2CH_2S)_3]^-$

Complexes *(1)* and *(3)* were found to be unreactive towards a range of mono- and di-substituted hydrazines. However, complex *(3)* did react cleanly with excess hydrazoic acid to give $[Mo_2O_2(\mu\text{-}N_3)(SCH_2CH_2CH_2S_3)]^-$. The reaction was carried out in the hope of generating nitrido-complexes by decomposition of azido-intermediates.

Hydrazoic acid was generated *in situ* by the reaction

0340-4285/90 $03.00 + .12

Table 1. Some mono- and dinuclear oxo-thiolato complexes of molybdenum.

Complex	Analysis[a] (%) C	H	N	ν(Mo=O)[b]	$\nu(N_3)$	λ_{max}[c]	ε[d]	m[e]
$[PPh_4][MoO(SCH_2CH_2S)_2]$ *(1)*	52.8 (52.9)	4.5 (4.4)		930	–	381	10,400	97.4
$[Et_4N][MoO(SCH_2CH_2S)_2]$ *(2)*	37.2 (37.0)	6.8 (7.0)	2.8 (3.1)	925	–	–	–	–
$[PPh_4][MoO(SCH_2CH_2CH_2S)_2]$ *(3)*	54.8 (54.3)	5.0 (4.9)		930	–	550	14,100	79.5
$[PXP][MoO(SCH_2CH_2CH_2S)_2]_2$ *(4)*	44.8 (45.2)	4.0 (4.2)		930	–	547	15,600	146.4
$[PPh_4][Mo_2O_2(\mu\text{-}N_3)(SCH_2CH_2CH_2S)_3]$ *(5)*	43.2	5.0	4.0	935	2035	395	41,800	93.6

[a]Calculated values in parenthesis; [b]Nujol mull spectra; [c]Absorbtion maxima nm, in acetonitrile solution; [d]Molar extinction coefficient, $mol^{-1}\,dm\,cm^{-1}$; [e]Molar conductivity, $ohm^{-1}\,cm^2\,mol^{-1}$.

Table 2. Convolution data for $[MoO(SCH_2CH_2S)_2]^-$.

$\nu(V\,s^{-1})$	$I_L(A\,s^{-1}) \times 10^{-5}$	dI_{pa}/dI_{pc}
0.05	4.6	1.0
0.1	4.3	1.0
0.2	4.3	1.0
0.5	4.5	0.98
1.0	4.5	0.96
2.0	4.0	0.95
5.0	4.4	0.90

of trimethylsilylazide (Me_3SiN_3) with methanol. Complex *(5)* is formed in good yield in methanol as an orange micro-crystalline solid and is soluble in acetonitrile or dichloromethane. The i.r. spectrum shows a strong single band at $930\,cm^{-1}$ assigned to ν(Mo=O) and a strong sharp band at $2035\,cm^{-1}$ attributed to $\nu(N_3)$. Charge transfer bands can be seen in the u.v. spectrum at considerably higher energy (*ca.* 350 nm) than that of its precursor complex. The ^1H n.m.r. spectrum is complex with several resonances between 2.2 and 3.9 ppm which are assigned to the methylene protons of the 1,3-propanedithiolate ligands. They appear as complicated multiplets reflecting the asymmetry of the dithiolate backbones and complex spin—spin splittings.

*The X-ray crystal structures of $[PPh_4][MoO(SCH_2CH_2CH_2S)_2]$ (1) and $[PPh_4][Mo_2O_2(\mu\text{-}N_3)(SCH_2CH_2CH_2S)_3]$ (5)**

Suitable crystals for an X-ray crystal structure of $[PPh_4][MoO(SCH_2CH_2CH_2S)_2]$ were grown from an acetonitrile-diethyl ether mixture. Relevant bond-lengths and angles are given in the legend for Figure 1, and full structural experimental data are listed in Table 3.

An ORTEP view of the anion $[MoO(SCH_2CH_2CH_2S)_2]^-$ (Figure 1) reveals an overall square pyramidal geometry. The oxo-ligand occupies an axial site, and the four thiolato-sulphurs form the basal plane from which the molybdenum is slightly displaced towards the oxo-group, giving the $MoOS_4$ core an overall C_{4v} symmetry. The displacement from the basal plane of the metal atom is also seen in the related complexes $[MoO(SPh)_4]^-$[2], $[ReS(SCH_2CH_2S)_2]^-$[9] and $[MoO(SCH_2CH_2S)_2]^-$[4]. This is attributed to electrostatic repulsions of the thiolato-sulphur lone pairs with the relatively electron rich M=X moiety (M = Re or Mo, $X = S^{2-}$ or O^{2-}).

The Mo—O bond distance (1.647(3) Å) is similar to that in $[MoO(SPh)_4]^-$ and longer than that found in $[MoOCl_4]^-$ (1.619(10) Å)[7]. This correlates with the i.r. spectroscopic data indicating that the electron donating thiolates weaken the M=O bond. The average Mo—S distance (2.389(3) Å) for *(3)* is, as expected, close to the value found in $[MoO(SCH_2CH_2S)_2]^-$ (2.372(3) Å)[4] indicating a small thiolate substituent effect.

Dark red crystals of $[PPh_4][Mo_2O_2(\mu\text{-}N_3)(SCH_2CH_2CH_2S)_3]$ *(5)* were grown from acetonitrile-diethyl ether. An ORTEP view of the anion is shown in Figure 2 together with a list of selected bond lengths and angles. Coordinates and details of the structural experimental data can be found in Table 3.

Complex *(5)* is dinuclear with two non-equivalent pseudo-octahedral molybdenums. The asymmetry is imposed by the odd number of chelated dithiolato-ligands two of which also provide bridging sulphurs for the Mo(1) atom while Mo(2) is ligated by another non-bridging chelated dithiolate. The bridging sulphur atoms have longer Mo—S distances (average 2.47(8) Å)

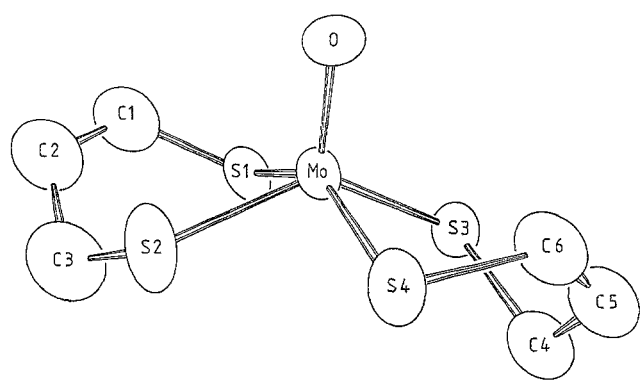

Figure 1. ORTEP representation of $[MoO(SCH_2CH_2CH_2S)_2]^-$ showing atom labelling scheme. Selected bond lengths (Å) and angles (°): Mo—O, 1.667(8), Mo—S1, 2.398(3); Mo—S2, 2.376(3); Mo—S3, 2.387(3); Mo—S4, 2.393(4); <S1—Mo—S2, 80.0(1); <S1—Mo—S3, 80.1(1); <S2—Mo—S4, 80.3(1); <S3—Mo—S4, 88.2(1); <S1—Mo—S4, 147.9(1); <S2— Mo—S3, 138.8(1).

* Atomic coordinates and displacment factor coefficients, full lists of bond lengths and angles and list of Fo/Fc values have been deposited with the Editor. Coordinates haves also been deposited with the Cambridge Crystallographic Data Centre.

Table 3. Experimental details for X-ray crystal structures of $[PPh_4][MoO(SCH_2CH_2CH_2S)_2]$ and $[PPh_4][Mo_2O_2(\mu\text{-}N_3)(SCH_2CH_2CH_2S)_3]$.

Crystal parameters at 21° C		
Compound	$[PPh_4][MoO(SCH_2CH_2CH_2S)_2]$	$[PPh_4][Mo_2O_2(\mu\text{-}N_3)(SCH_2CH_2CH_2S)_3]$
Mwt, g	663.74	923.89
a, Å	9.612(2)	9.398(3)
b, Å	21.022(4)	14.650(2)
c, Å	15.462(3)	25.426(2)
α, deg	90	90
β, deg	103.06(1)	90
γ, deg	90	90
V, Å^3	3043.3	3775.8
Space group	P_{2_1}/n	$P_{2_12_12_1}$
Z	4	4
D_{calc}, g/cm^3	1.45	1.62
F(000)	1364.0	1872
μ, cm^{-1}	7.64	–

Measurement of Intensity data		
Compound	$[PPh_4][MoO(SCH_2CH_2CH_2S)_2]$	$[PPh_4][Mo_2O_2(\mu\text{-}N_3)(SCH_2CH_2CH_2S)_3]$
Instrument	Nicolet R3m	
Radiation	Mo K_α ($\lambda = 0.710$ Å)	
Scan Mode	Coupled θ (crystal) – 2θ (counter)	
Scan Route	Variable within limits 6° to 30°/min	
Scan Range	$0° < 2\theta < 45°$	
Scan Length	$[2\theta(k_{\alpha 1}) - 1.0]°$ to $[2\theta(k_{\alpha 2}) + 1.0]$	
Background Measurements	Stationary crystal, stationary counter at the beginning and end of each 2θ scan; each measurement for half the time taken for the 2θ scan	
Standards	3 measured every 197 data reflections	3 measured every 147 data reflections
Number of reflections collected	3687	2563
Number of independent reflections used in solution	1957 with $I_\sigma > 3\sigma(I_0)$	1244 with $I_\sigma > 3\sigma(I_0)$

Data Reduction and Structure Solution[b]		
Compound	$[PPh_4][MoO(SCH_2CH_2CH_2S)_2]$	$[PPh_4]Mo_2O_2(\mu\text{-}N_3)(SCH_2CH_2CH_2S)_3]$
Absorption Coefficient (cm^{-1})	7.64	10.42
Absorbtion Correction	None ($T_{max}/T_{min} = 1.08$)	None ($T_{max}/T_{min} = 1.13$)
Structure solution	Mo position located from three dimensional Patterson map. All other non-hydrogen atoms located on subsequent difference Fourier synthesis. Hydrogen atoms included in final stages of refinement on fixed contributors in idealised positions	
Atomic Scattering Factors	Neutral atomic scattering factors were used throughout the analysis	
Anomalous Dispersion[d]	Applied to all non-hydrogen atoms	
Final Discrepancy Factor[e]	$R = 0.058$	$R = 0.058$
	$R_w = 0.060$	$R_w = 0.055$
Goodness of fit	1.65	1.10

[a]From a least squares fitting of the setting angle of 25 reflections; [b]all calculations were performed on a Data General Nova 3 computer with 32 K of 16-bit words using local version of the Nicolet SHELXTL interactive crystallographic software package as described in G. M. Sheldrick "Nicolet SHELXTL Operations Manual", Nicolet XRD Corp. Cupertino, CA 1970 U.S.A., [c]D. T. Cramer and J. B. Mann, *Acta Cryst. (A)*, **24**, 321 (1968); [d]*International Tables for X-ray Crystallography*, Vol. III, Kynoch Press, 1962; [e]$R = \sum[|F_o| - |F_c|/\sum|F_o|]$; $R_w = [\sum w(|F_o| - |F_c|)^2/\sum w|F_o|^2]^{1/2}$; $w = 1/\sigma^2(F_o) + g^*(F_o)^2$ $g = 0.001$, [f]$GOF = [\sum w(|F_o| - |F_c|)^2/(NO—NV)^{1/2}$ where NO is the number of observations and NV is the number of variables.

than the terminal ligands (average 2.40(8) Å). The oxygen atoms are terminally co-ordinated with similar Mo(1)—O(1) and Mo(2)—O(2) distances of 1.67(1) Å and 1.66(1) Å respectively. These distances are similar to those found in complex *(3)*.

The azide group and two thiolato-sulphur atoms make up the triple bridge. The most interesting feature of this unit is the non-linear conformation of the azide group which is bent at N(2) with N(1)—N(2)—N(3) = 153.4(29)°. The non-linearity is caused by an intermolecular interaction of the N(3) nitrogen with a methylene hydrogen of an adjacent molecule within the unit cell and is not electronic in origin. The difference in N—N bond lengths [N(1)—N(2) (1.18(2) Å) and N(2)—N(3)

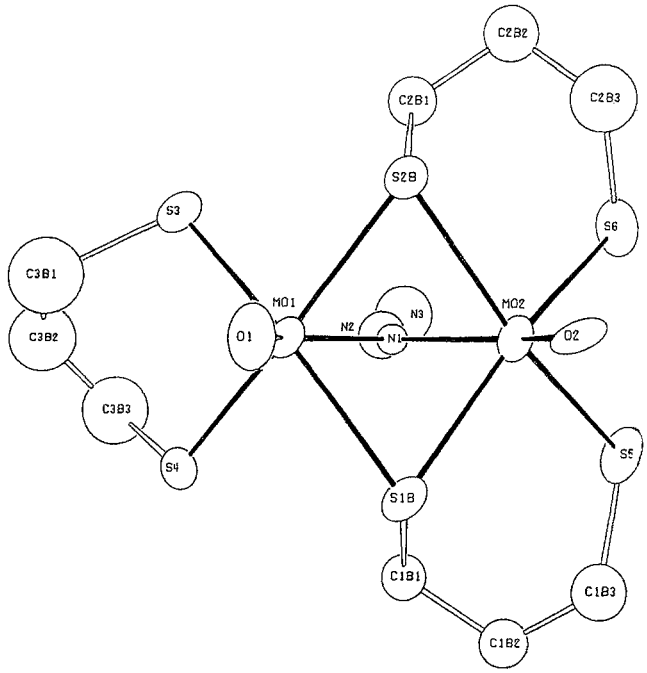

Figure 2. ORTEP representation of $[Mo_2O_2(\mu\text{-}N_3)(SCH_2CH_2CH_2S)_3]^-$ showing atom labelling scheme. Selected bond lengths (Å) and angles (°):- Mol—Mo2, 2.893(3); Mol—O1, 1.67(1); Mo2—O2, 1.66(1); Mol—N1, 2.21(1); Mo2—Nl, 2.24(1); Nl—N2, 1.18(2); N2—N3, 1.09(4). < S1B—Mol—S3, 164.8(3); < S2B—Mol—S4, 164.2(3); < O1—Mol—Nl, 153.8(8); < S3—Mol—S4, 76.0(3); < S1B—Mo2—S5, 87.2(3); < N1—N2—N3, 153.4(29).

(1.09(4) Å)] is typical of that found in other terminally coordinated azide groups[10]. In contrast, the Mo(1)—N(1) and Mo(2)—N(1) bond distances of 2.21(1) Å and 2.24(1) Å respectively are long compared to those of other terminal or bridging azido-ligands[10] (1.943(5)–2.121(14) Å). The long Mo—N bond distances are probably due to the azido-ligands being *trans* to the oxo-ligands, which exert a high *trans* influence.

The structural parameters for the triple bridge are very similar to those found in other triply-bridged oxo-molybdenum(V) species such as $[Mo_2O_2Cl_5(SPh)_2]^-$[11], $[Mo_2O_2Cl(SPh)_2(S_2CNEt_2)_2]^+$[12] and $[Mo_2O_2(SPh)_2(S_2CNEt_2)_2]$[11]. All contain a MoS_2Mo moiety in the bridge with a hetero-ligand occupying the third bridging site. Interestingly these structurally analogous complexes have Mo—Mo distances in the range 2.649(1) Å to 2.915(1) Å[11] which compares with 2.890(3) Å for complex *(5)*. The Mo—S—Mo angles in *(5)* are acute (approximately 75°) as a consequence of the metal–metal interaction.

Electrochemistry

Convolution analysis

Treatment of electrochemical data obtained by cyclic voltammetry has previously involved analysis of the region associated with the current peak heights centred at E_p or $E_{1/2}$ values[13]. Analysis of this region can give an indication of the reversibility of the electrode process. Previous workers[14,15,16] have utilized an alternative method of analysis involving convolution transform. Here an assessment is made of the whole cyclic voltammogram which permits a sensitive quantitative assessment of both electrode (heterogeneous) and chemical (homogeneous) kinetics. Taylor *et al.* have demonstrated the scope of this technique in a recent paper[13]. Here we report the application of convolution analysis to some electrode processes involving Nernstian behaviour utilizing recently available commercial software[17].

For a Nernstian electron transfer process convolution (I_1) of the current i with a function $(\pi t)^{-1/2}$ is obtained from the whole current history i(u);-

$$I_1 = \frac{1}{\pi^{1/2}} \int_0^t \frac{i(u)}{(t-u)^{1/2}} du$$

where I_1 is the convolution transform function. Consequently for reversible electrochemical behaviour the $E_{1/2}$ potential is related by:-

$$E = E_{1/2} + \frac{RT}{nF} \frac{I_L - I_1}{I_1}$$

where I_L is the limiting convoluted current, i.e. where the initial concentration of the bulk species, [0]* at the electrode surface approaches zero, defined by

$$I_L = nFaD_0^{1/2}$$

where D_0 is the diffusion coefficient of species 0.

Typically I_1 will retrace itself on forward and backward scans and plots of $\ln [(I_L - I_1)/I_1]$ *versus* E will be linear with an intercept (x-axis) at $E_{1/2}$, the slope will correspond to RT/nF and I_L will be invariant with scan rate. The first derivative of I_1 with respect to time (dI_1/dt) is known as the deconvolution current. For reversible or Nernstian processes the plot of (dI_1/dt) *versus* E is symmetrical with both maxima at $E_{1/2}$ and the peak height ratio is close to unity.

Results

A typical cyclic voltammogram for $[MoO(SCH_2CH_2S)_2]^-$ is shown in Figure 3. An apparently reversible reduction process occurs followed by a further irreversible process. The first process corresponds to the formation of Molybdenum(IV) $[MoO(SCH_2CH_2S)_2]^{2-}$ but attempts to prepare this species by controlled potential reduction were not successful due to slow decomposition over the time scale of the experiment. The irreversible step appeared to involve two electrons based on peak current height but was not further studied.

Convolution analysis of the first reduction process of complex *(1)* $[(MoO(SCH_2CH_2S)_2]^-$ was carried out over the scan range 0.01 to 5.0 volts sec^{-1}. Some of these data are summarised in Table 2 and a typical reversible portion of the cyclic voltammogram is shown in Figure 4 together with its I_1 convolution transform. Figure 5 illustrates the corresponding (dI_1/dt) *versus* E plot.

The data in Table 2 indicate that I_L is essentially independent of scan rate suggesting the absence of homogenous chemical kinetic processes. This is substantiated by the virtual overlap of I_1 on the forward and backward scans except at extremes of scan rate. The deviations at slow scan rate are presumably due to marginal decomposition of the di-anion. At fast scan rates changing effects within the electrical double layer are probably responsible for the deviation from ideal behaviour. The (dI_1/dt) *versus* E plot (Figure 5) is completely symmetrical with maxima occurring at the

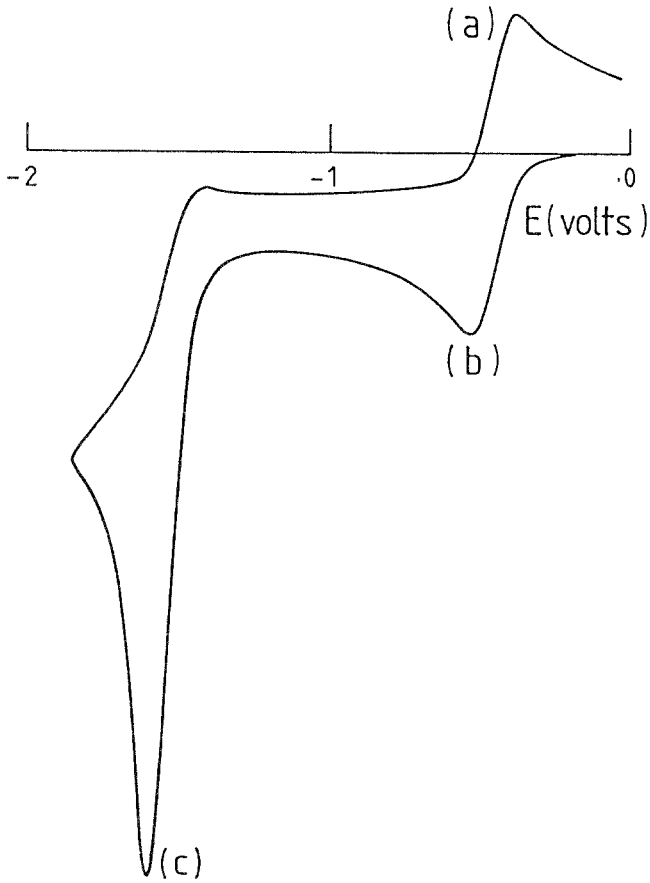

Figure 3. Cyclic voltammogram of complex *(1)*, together with its convolution transform, scan rate 0.5 V s^{-1}, Pt, 0.2 M $[NBu^n_4][BF_4]$-acetonitrile.

same potential. This is characteristic of diffusion controlled fast electron transfer unlimited by slow heterogeneous electron transfer kinetics. The half peak widths are about 105 mV regardless of scan rate which is within the range expected for a one electron process. The theoretical value for transfer of one electron is 92 mV.

Finally a plot of $\ln[(I_L - I)/I_1]$ *versus* E is a straight line with a slope of 37.5 V^{-1}. The slope of this plot for a Nernstian process is nF/RT which at 20° C for a one electron process has a value of 38.9 V^{-1}, in good agreement with the experimental value. The intercept on the E axis is −0.615 V which corresponds to $E_{1/2}$.

In summary, all the convolution data confirm that the primary reduction of $[MoO(SCH_2CH_2S)_2]^-$ is a diffusion controlled one electron process.

Experimental

C, H and N analyses were carried out by Mrs. G. Olney (University of Sussex). ^{1}H n.m.r. spectra were recorded using a JEOL FX90Q instrument at 90 MHz at ambient temperature with TMS as internal standard. I.r. spectra were obtained in Nujol mulls between KBr discs using a Pye Unicam SP2000 spectrophotometer in the range 400–4000 cm^{-1}. Electronic spectra in MeCN solution were recorded on a Pye Unicam SP1800 spectrophotometer. Conductivity measurements were made in MeCN solution using a Portland Electronics Conductivity bridge.

1,2-ethanedithiol and 1,3-propanedithiol were purchased from Aldrich and used without further purification. Synthesis of $[MoO_2\{(Me)CHOHCHO(Me)\}_3]\cdot 2(Me_3)CHOHCHOH(Me)$ was carried out according to the literature method[18]. Trimethylsilylazide was used as purchased from BDH.

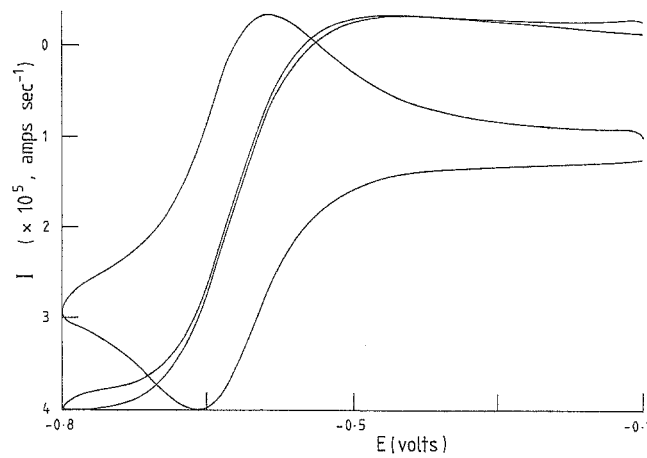

Figure 4. Reversible reduction process for complex *(1)* together with I_1 convolution transform.

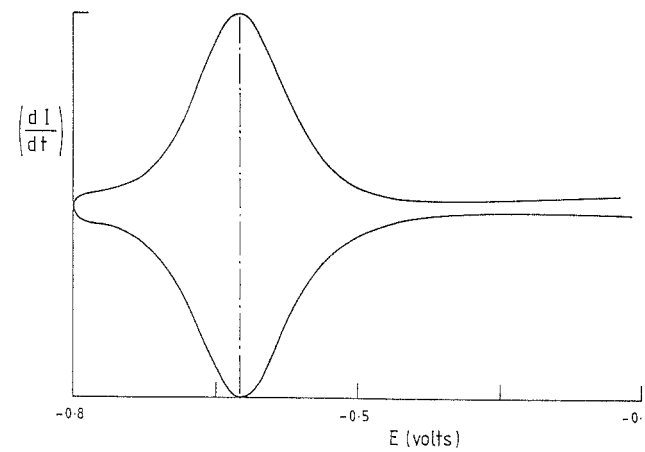

Figure 5. The deconvolution transform (dI/dt) from the convoluted data obtained from the cyclic voltammogram.

Cyclic voltammetry was carried out in dry MeCN/0.2 M $[Bu^n_4N][BF_4]$ under N_2 using a three electrode cell configuration at 21° C. The working electrode was a vitreous carbon disc with a measured surface area of 0.0706 cm^2. A platinum gauze counter electrode was used together with a silver wire pseudo-reference electrode arranged such that a luggin capillary was in close proximity to the working electrode. $E_{1/2}$ potentials are quoted *versus* the saturated calomel electrode, S.C.E., against which the ferrocenium/ferrocene couple has an $E_{1/2}$ value at 0.54 V in thf − 0.2 M $[Bu^n_4N][BF_4]$.

Cyclic voltammetric measurements were made on a Chemical Electronics Waveform Generator and a Hi-Tek Instruments Potentiostat, OT2101. Convolution analysis and cyclic voltammetric data associated with this were carried out using an EG and G model 362 scanning potentiostat. The current and potentials responses were stored on a magnetic disc *via* an EG and G twin channel 12-bit analogue-to-digital converter (50 μs conversion

time). Data were manipulated on an Opus microcomputer using EG and G's CONDECON 300(TM) software, version 2.0. Typically 500 data points were collected, background data were subtracted from sample data and positive feedback was applied *via* the potentiostat to the cell to minimize internal cell resistance.

Tetraphenylphosphonium bis(1,2-ethanedithiolato)-oxomolybdate(V) $[PPh_4][MoO(SCH_2CH_2S)_2]$ (1)

Triethylamine (2 cm^3, 16 mmol) was added to a solution of $[MoO_2(MeCHOHCHOMe)_2]$ (5 g, 10 mmol) in MeOH (50 cm^3) followed by 1,2-ethanedithiol (4.7 g, 50 mmol). The clear solution quickly became green-blue in colour. Addition of tetraphenylphosphonium bromide (5 g, 12 mmol) gave a green-blue crystalline precipitate which was immediately filtered off under suction (4.6 g, 70% yield).

Tetraethylammonium bis(1,2-ethanedithiolato)-oxomolybdate(V) $[Et_4N][MoO(SCH_2CH_2S)_2]$ (2)

Complex *(2)* was prepared in an analogous manner to *(1)*, except tetraethylammonium chloride was added (3.20 g, 74% yield).

Tetraphenylphosphonium bis(1,3-propanedithiolato)-oxomolybdate(V), $[PPh_4][MoO(SCH_2CH_2CH_2S)_2]$ (3)

Complex *(3)* was prepared in an analogous manner to *(1)*, except 1,3-propanedithiol (5.4 g, 50 mmol) was added. (5.2 g, 78% yield). Crystals of *(3)* suitable for X-ray analysis were obtained from MeCN—Et_2O.

1,2-benzylbis(triphenylphosphonium) bis(1,3-propanedithiolato)oxomolybdate(V), $[PXP][MoO(SCH_2CH_2CH_2S)_2]_2$ (4)

Complex *(4)* was prepared in an analogous manner to *(3)*, except 1,4-benzylbis(triphenylphosphonium)dibromide (1 g, 1.3 mmol) was added (3.81 g, 57% yield).

Tetraphenylphosphonium (μ-azido)(μ-1,3-propanedithiolato) bis(1,3-propanedithiolato)bis(oxo)-dimolybdate(V), $[PPh_4][Mo_2O_2(\mu\text{-}N_3)(SCH_2CH_2CH_2S)_3]$, (5)

To a suspension of $[PPh_4][MoO(SCH_2CH_2CH_2S)_2]$ *(3)* (1 g, 1.5 mmol) in MeOH (30 ml) was added Me_3SiN_3 (0.18 g, 1.5 mmol) (HN_3 generated *in situ*). The reaction mixture was allowed to stir overnight, by which time a red-orange micro-crystalline solid had precipitated from the pale red solution. The solid was filtered and dried *in vacuo* (0.32 g, 63% yield).

Acknowledgements

Two of us (P.T.B. and J.R.D.) thank the AFRC Unit of Nitrogen Fixation for provision of laboratory facilities and financial support for part of this work and to Dr. N. Taylor (University of Leeds) for helpful discussions concerning the convolution analysis of the electrochemical data.

References

(1) G. Hanson, A. A. Brunette, A. C. MacDonald, K. S. Murray and A. G. Wedd, *J. Am. Chem. Soc.*, **103**, 1953 (1981).
(2) I. W. Boyd, I. G. Dance, K. S. Murray and A. G. Wedd, *Aust. J. Chem.*, **31**, 2423 (1978).
(3) R. J. Burt, G. J. Leigh, J. R. Dilworth and J. A. Zubieta, *J. Chem. Soc. Dalton Trans.*, 2295 (1982).
(4) S. R. Ellis, O. Collison, C. D. Garner and W. Clegg, *J. Chem. Soc. Chem. Commun.*, 1483 (1986).
(5) P. T. Bishop, J. R. Dilworth, J. Hutchinson and J. A. Zubieta, *J. Chem. Chem. Commun.*, 1053 (1982).
(6) I. W. Boyd, I. G. Dance, A. E. Landors and A. G. Wedd, *Inorg. Chem.*, **18**, 1875 (1979).
(7) C. D. Garner, L. H. Hill, F. E. Mabbs, F. E. McFadden and A. T. McPhail, *J. Chem. Soc. Dalton Trans.*, 853 (1974).
(8) P. M. Boormanm, C. D. Garner, F. E. Mabbs and T. J. King, *J. Chem. Soc. Chem. Commun.*, 663 (1974).
(9) P. J. Blower, J. R. Dilworth, J. Hutchinson and J. A. Zubieta, *J. Chem. Soc. (Dalton)*, 1339 (1986).
(10) Z. Dori and R. F. Ziolo, *Chem. Rev.*, **97**, 1616 (1975).
(11) J. R. Dilworth, B. D. Neaves, P. Dalstrom, J. Hyde and J. A. Zubieta, *Trans. Met. Chem.*, 7, 257 (1982).
(12) G. Benzey, J. H. Enemark, J. I. Gelder and K. Yamanouchi, in P. C. Metchell and J. Seaman, (Eds.), Proceedings, Second International Conference on Chemistry and Uses of Molybdenum, Climax, Michigan (1977) p. 50.
(13) R. S. Nicolson and I. Shain, *Anal. Chem.*, **36**, 706 (1964).
(14) A. Blagg, S. W. Carr, G. R. Cooper, I. Dobson, J. Bernard Gill, D. C. Goodall, B. L. Shaw, N. Taylor and T. Boddington, *J. Chem. Soc. Dalton Trans.*, 1213 (1985) and references therein.
(15) F. E. Woodward, R. O. Goodin and P. J. Kinlen, *Anal. Chem.*, **56**, 1920 (1984).
(16) J. C. Imbeaux and J. M. Savéant, *Electroanal. Chem.*, and *Interfacial Electrochem.*, **44**, 169 (1973).
(17) E. G. and CONDECON 300(TM) Version 2.0.
(18) R. J. Butcher, H. K. J. Powell and S. M. Yong, *J. Chem. Soc. Dalton Trans.*, **356** (1976).

(Received 31 May 1989) TMC 2100